



Morphology and mechanical properties of bisphenol A polycarbonate/poly(styrene-co-acrylonitrile) blends based clay nanocomposites

Demiao Lin^{a,b,c}, Adriana Boschetti-de-Fierro^{a,1}, Michaël Alexandre^{a,d}, Clarissa Abetz^a, Heinrich Böttcher^a, Volker Abetz^{a,*}, Laetitia Urbanczyk^d, Christine Jérôme^d, Charles C. Han^b

^a Institute of Polymer Research, Helmholtz-Zentrum Geesthacht, 21502 Geesthacht, Germany

^b State Key Laboratory of Polymer Physics and Chemistry, Joint Laboratory of Polymer Science and Materials, Institute of Chemistry, Chinese Academy of Sciences, Beijing 100190, China

^c Graduate School of the Chinese Academy of Sciences, Beijing 100049, China

^d Center for Education and Research on Macromolecules (CERM), University of Liège, Sart-Tilman B6a, 4000 Liège, Belgium

ARTICLE INFO

Article history:

Received 16 March 2011

Received in revised form 8 September 2011

Accepted 9 September 2011

Available online 16 September 2011

Keywords:

A. Nano composites

A. Polymers

B. Mechanical properties

E. Extrusion

ABSTRACT

Two organic modified clays (Cloisite®30B (CL30B) and PCL/Cloisite®30B masterbatch (MB30B)) were used to improve the mechanical properties of polycarbonate (PC)/poly(styrene-co-acrylonitrile) (SAN) blends. Transmission electron microscopy (TEM) and X-ray diffraction (XRD) measurements of the melt blended nanocomposites revealed that partially exfoliated and partially degraded structure was obtained and the clay platelets were located mostly in the SAN phase and at the two-phase boundary. Dispersion of the clay platelets is better when MB30B were used. The mechanical properties of the clays filled nanocomposites vary accordingly and when MB30B is used better mechanical properties can be achieved. Tensile strength increases 41% at maximum as the CL30B loading is 5 wt.%, while elongation at break decreases dramatically. Impact strength can be improved up to 430% compared to the pure blend when 1 wt.% MB30B was used.

© 2011 Published by Elsevier Ltd.

1. Introduction

Polymer-layered silicate nanocomposites (PNCs) are composite materials in which small amount of mineral clay particles with a thickness in the nanometer range are dispersed randomly and homogeneously in a polymer matrix [1–5]. Due to high specific surface area of the dispersed nanoparticles, mechanical, thermal and barrier properties of the filled nanocomposites can be enhanced compared to the ones of pristine polymers [6,7]. The challenge in preparing high performance PNC is to efficiently delaminate the clay sheets and disperse the sheets properly in the polymer matrix. Solvent intercalation, *in situ* polymerization intercalation and melt blending are the most popular methods to incorporate the layer crystal to the host polymers [6,7]. From an application point of view, the latter is of higher importance than the others and therefore it is often used in industry. Only in a few cases, one can obtain fully exfoliated and well dispersed clay sheets in a polymer matrix, for example in Nylon-6-organoclay nanocomposites [6,7].

In the case of polymer blend nanocomposites (PBNCs), the ultimate properties of PBNCs are strongly influenced by the domain

structure, size, and interfacial interaction [8–15]. During the addition of clay into the polymer blend system, the coalescence of the droplets can be suppressed if the clay platelets are located at the phase boundary of the two polymers [16]. Meanwhile, the interfacial interaction between the immiscible phases can be enhanced.

In the present work we focus on the influence of two organic modifications of the clay surface and of the clay loading on the structure and mechanical properties of nanocomposites based on PC/SAN blends. Because incorporation of organo-modified clay into bisphenol A polycarbonate [17] and poly(styrene-co-acrylonitrile) [18] was found to form a highly exfoliated structure, we believe the clay platelets may locate at the phase boundary of the blend components when incorporated under certain conditions and enhance the interfacial strength. For this purpose, PC/SAN PBNCs have been prepared by melt blending. The structure and mechanical properties of these nanocomposites were systematically studied by microscopy, scattering and mechanical test methods.

2. Material and methods

2.1. Materials

SAN, having an acrylonitrile content of 25 wt.%, weight average molecular weight (\bar{M}_w) of 1.7×10^5 g/mol, was purchased from Sigma-Aldrich, Germany. Two kinds of bisphenol A polycarbonate,

* Corresponding author. Tel.: +49 0 4152 87 1536; fax: +49 0 4152 87 2499.

E-mail address: Volker.Abetz@hzg.de (V. Abetz).

¹ Present address: Gambro Dialysatoren GmbH, Research and Development, Holger-Crafoord-Str. 26, 72379 Hechingen, Germany.

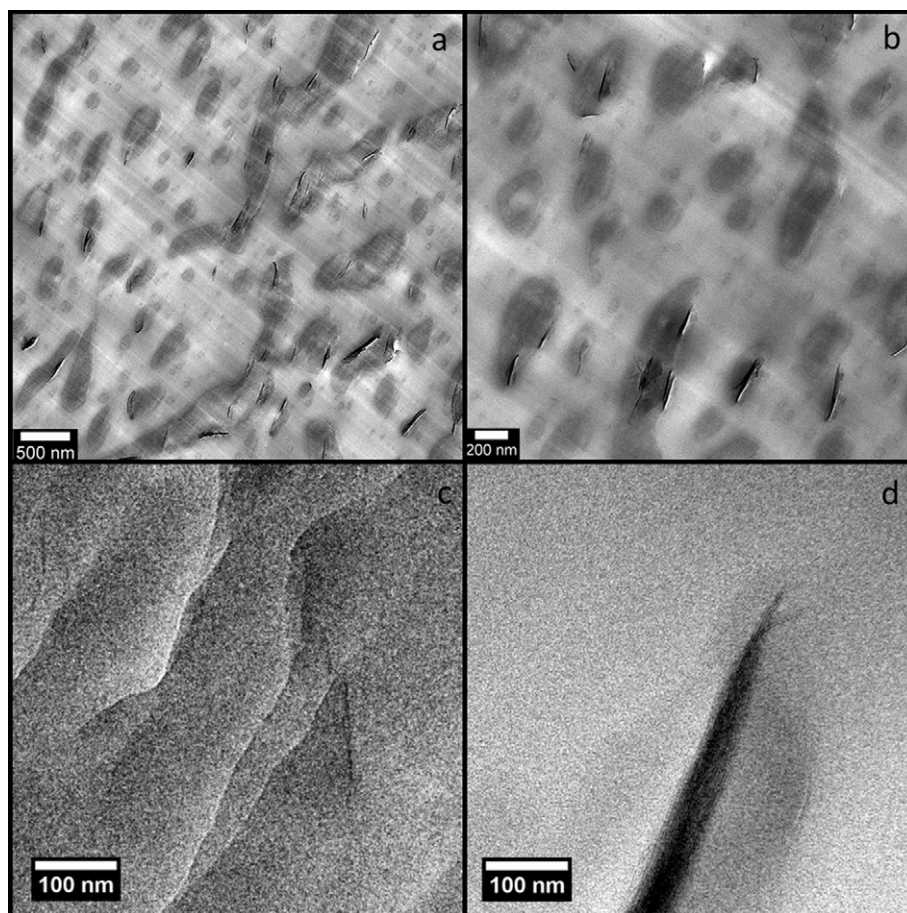


Fig. 1. TEM images of HPC/SAN 7/3 1 wt.% MB30B at different magnifications.

with different melt indices of 7 g/10 min (300 °C/1.2 kg) (LPC) and 10–12 g/10 min (300 °C/1.2 kg) (HPC) were obtained from Sigma-Aldrich too. Weight average molecular weights of 5.4×10^4 g/mol (HPC) and 6.1×10^4 g/mol (LPC) were obtained from GPC measurements using polystyrene as standard. Cloisite®30B (CL30B) from Southern Clay Products (TX, USA) is a commercial montmorillonite organo-modified with bis-(2-(hydroxyethyl) methyl (tallowalkyl) ammonium cation. PCL/Cloisite®30B masterbatch (MB30B) were prepared by *in situ* polymerization of ϵ -caprolactone in supercritical carbon dioxide [18,19]. The inorganic fractions of CL30B and MB30B are 80 wt.% and 53 wt.% respectively. The number average molecular weight (\bar{M}_n) of PCL in MB30B is 1.5×10^3 g/mol determined by GPC using polystyrene as standard. These short PCL chains are not able to entangle with the SAN matrix chains [18]. PC/SAN PBNCs with clay loading of 1 wt.%, 2 wt.% and 5 wt.% were prepared, in which the weight fractions of clay are related to naked clay. For MB30B PBNCs the 5 wt.% composition is missing since the specimen is too brittle and cannot be shaped.

2.2. Melt-blending process

PC was dried at 120 °C under vacuum for more than 8 h. SAN was dried at 100 °C under vacuum for more than 4 h. CL30B and MB30B were used as received. The clays were melt blended with the molten HPC/SAN 7/3 (LPC/SAN 7/3) matrix in a mini-twin screw extruder (DSM, Netherlands) at a barrel temperature of 230 °C (240 °C for LPC/SAN 7/3), screw rotation speed 50 rpm for

5 min. Specimens for tensile and impact test were injection molded and the mold temperature was 100 °C.

2.3. Characterization

XRD spectra were obtained in a Rigaku D/max2500 powder diffractometer from 2 °C to 10 °C at room temperature using Cu K α radiation.

The tensile properties of all the specimens had been measured in accordance to standard ASTM D638 in a Zwick/Roell tensile tester at a test speed of 10 mm/min at 25 °C. Charpy impact properties were measured in Zwick/Roell impact tester at 25 °C. At least five specimens were used for each test. The average values and the errors were calculated. The morphology of the PBNCs was observed by TEM (Tecnai G2 F20, 200 kV, bright field mode). Ultrathin specimens were prepared by an ultramicrotome (Reichert Jung) and used without staining because the contrast between different components was high enough.

3. Results and discussion

3.1. Morphology

For both kinds of clays used here, most of the clay platelets are located in the SAN minority phase and in the phase boundary of PC/SAN blends. Fig. 1 shows the TEM images of HPC/SAN 7/3 blend containing 1 wt.% MB30B, which clearly indicates that most of the

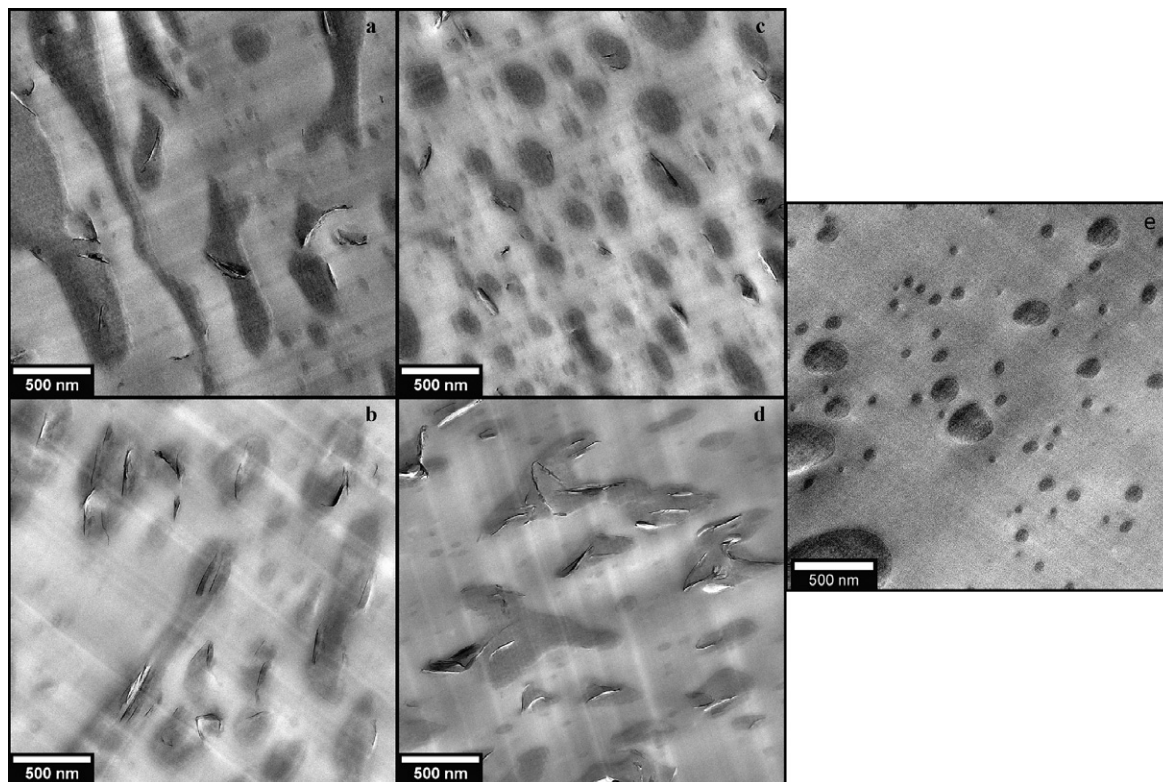


Fig. 2. TEM images of (a) HPC/SAN 7/3 1 wt.% CL30B; (b) HPC/SAN 7/3 1 wt.% MB30B; (c) HPC/SAN 7/3 2 wt.% CL30B; (d) HPC/SAN 7/3 2 wt.% MB30B; (e) HPC/SAN 7/3.

clay particles are well dispersed in the SAN matrix although some form primary particles with dimensions in the micrometer range. Part of the clay platelets locate around the two-phase boundary of PC and SAN, as it is clearly shown in Fig. 1a and b. One to several platelets is separated from each other (their lengths range from 100 nm to 300 nm); while some other clay platelets are still aggregated in primary particles. In Fig. 1c, exfoliated clay platelets can be clearly observed while stacked clay structure is observed in Fig. 1d. Fig. 2 shows the TEM images of HPC/SAN 7/3 PBNCs with both modified and unmodified fillers and different filler loading. The dispersed SAN domains appear darker than the PC matrix. From Figs. 1 and 2, it is clear that all the PBNCs have similar structures: clay particles are located in the SAN domains and two phase boundary; partial exfoliation structure exists at least in the MB30B PBNCs.

Fig. 3 shows the XRD patterns of HPC/SAN 7/3 blends, CL30B, MB30B and their PBNCs. The XRD results show that there is one peak in PBNCs filled with CL30B except HPC/SAN 7/3 blend with 5 wt.% CL30B. The interlayer distance of PBNCs corresponding to high 2θ values decreases from 1.8 nm to 1.5 nm compared to that of pure CL30B. The intensity of PBNCs at 1.5 nm is high compared to the intensity of pure CL30B at 1.8 nm because the XRD profiles of PBNCs were obtained from the skins of the injection-molded bars. The alignment of the clay particles in the skin is expected to enhance the reflection peak height [20,21].

The XRD signals at 3.7 nm of HPC/SAN 7/3 5 wt.% CL30B and HPC/SAN 1 wt.% MB30B are probably fake signals which may come from the incident beam instead of the basal reflections arising from the layered silicates because the detector is too close to the incident beam. The broad and very weak peak (shoulder) of HPC/SAN 7/3 5 wt.% CL30B XRD profile near $2\theta = 3.5^\circ$ is visible, which is typical for a disordered system with partial exfoliation structure [18]. In the PBNCs filled with 2 wt.% MB30B there are two diffraction peaks corresponding to interlayer space values of 1.5 nm and 3.0 nm (the interlayer space for pure MB30B is 3.2 nm). The de-

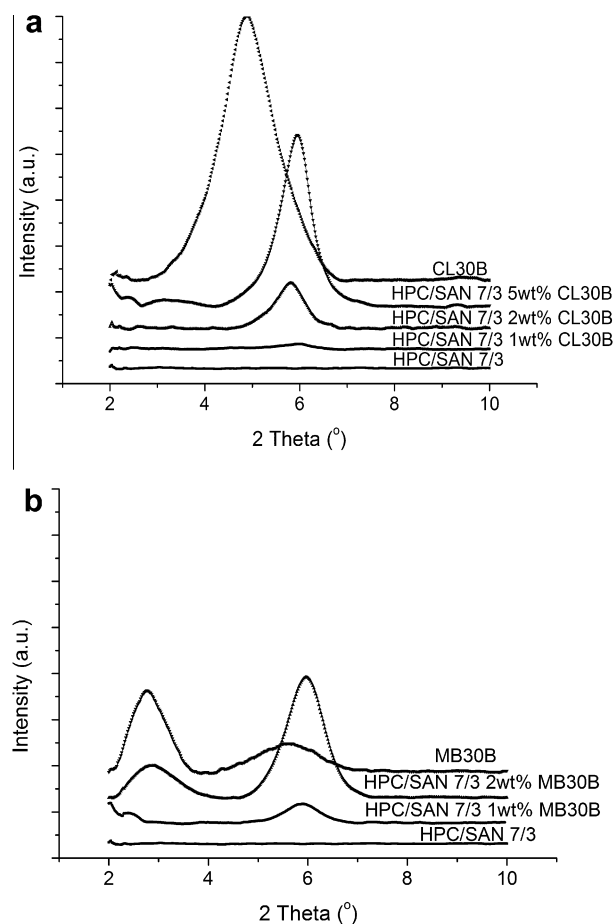


Fig. 3. XRD patterns of: (a) HPC/SAN 7/3 CL30B PBNCs and (b) HPC/SAN 7/3 MB30B PBNCs.

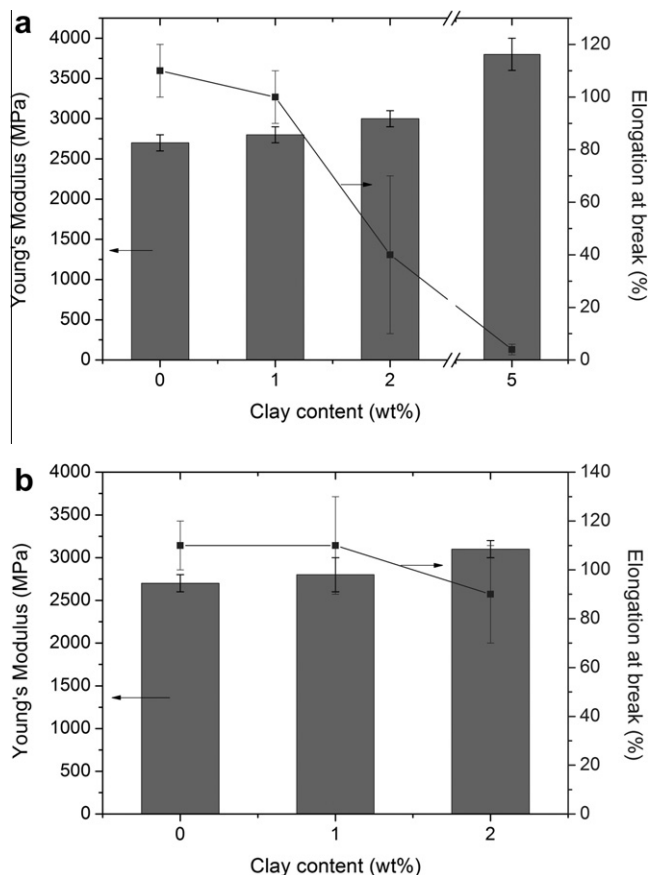


Fig. 4. Tensile properties as a function of clay content of: (a) HPC/SAN 7/3 CL30B PBNCs and (b) HPC/SAN 7/3 MB30B PBNCs.

crease in interlayer space may be caused by the degradation of the organic component of the filler during processing [22]. The more pronounced diffraction peak at low scattering value in MB30B filled PBNCs implies that in MB30B there remains more undegraded clay than in CL30B.

3.2. Mechanical properties

Compared to HPC/SAN 7/3 blends, Young's modulus of HPC/SAN 7/3 CL30B PBNCs increased by 4%, 11% and 41% on average when the clay loading increased from 1 wt.%, 2 wt.% to 5 wt.%, respectively (see Fig. 4a). This is because the increase of clay loading led to an increase of exfoliated component in the SAN phase probably due to the increase in shear forces during extrusion. The increase in exfoliation enhances the total interaction between the clay platelets and polymer matrix. However, elongation at break of the same materials decreased from 91%, 36% to 4% at the same time.

When comparing different clays, Young's modulus of HPC/SAN 7/3 MB30B PBNCs (2 wt.% clay loading) increased by 15% which was slightly more than HPC/SAN 7/3 CL30B PBNCs (2 wt.% clay loading), which was caused by better dispersion of MB30B (see Fig. 4b). The elongation at break of HPC/SAN 7/3 MB30B PBNCs and HPC/SAN 7/3 CL30B PBNCs decreased as the clay content increased. Again, PBNCs filled with MB30B obtained better elongation at break results due to the fact that the dispersion of filler was better.

For LPC/SAN7/3 PBNCs, qualitatively similar results were obtained and therefore are not discussed further.

Charpy impact properties showed that the maximum increase of impact strength was obtained when the clay loading was about

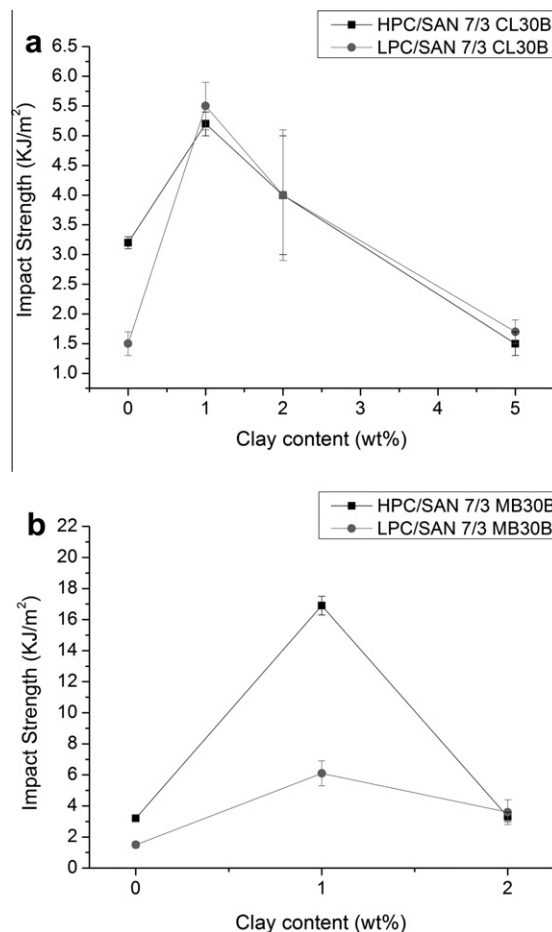


Fig. 5. Impact strength as a function of clay content of: (a) CL30B PBNCs and (b) MB30B PBNCs.

1 wt.% (see Fig. 5). Then the impact strength tended to decrease as the clay loading increased. The maximum impact strength obtained in HPC/SAN 7/3 1 wt.% MB30B PBNCs was about 430% higher than the value corresponding to the pure HPC/SAN blend. Note that when 1 wt.% of MB30B was filled into HPC/SAN 7/3 blends the impact strength increases dramatically while the Young's modulus increases slightly and the elongation at break remains close to that of the pure blend (91% of pure blend). This may be caused by better dispersion of clay platelets that leads to an increased amount of platelets located at the phase boundary. As the clay loading increased further, the defects introduced by the filler in the system also increase which leads to a decrease of the nanocomposites' toughness. The influence of PCL on the mechanical properties of PC/SAN 5/5 blend was reported by Kim and Lee [23]. The Notched Izod impact properties can be improved only when the PCL content is higher than 20 wt.%. The PC/SAN composition 7/3 in our work is different from the composition 5/5 in the publication, and the PCL content needed to improve the impact properties of PC/SAN 7/3 should be different. In HPC/SAN 1 wt.% MB30B PBNCs, the PCL content is only 0.89 wt.% which is too small to have such a huge toughening effect on HPC/SAN 1 wt.% MB30B PBNCs.

4. Conclusions

From this study, no significant differences in the morphology were observed for the two kinds of clay used, since all the clay platelets located mainly in the SAN phase and at the phase boundary of PC/SAN blends. Partially exfoliated structures were found in

these nanocomposite materials which were verified by TEM and XRD measurements. Young's modulus tended to increase when the clay loading increased. MB30B clay, which has a larger amount of organic component, can disperse better in the matrix and enhances tensile properties and impact strength better than CL30B clay. The impact strength of MB30B filled PBNCs can be dramatically increased when the clay loading is about 1 wt.%, while Young's modulus and elongation at break remain in the same level of the pure blends. This can extend the potential application of PC/SAN based nanocomposites.

Acknowledgements

Financial supports from German Academic Exchange Service (DAAD) and Chinese Academy of Sciences (CAS) are gratefully acknowledged. CERM thanks the "Belgian Federal Government Office Policy of Science (BELSPO)" for general support in the frame of the PAI-6/27.

References

- [1] Usuki A, Hasegawa N, Kato M, Kobayashi S. Polymer-clay nanocomposites. *Inorg Polym Nanocompos Membr*, vol. 179. Berlin, Heidelberg: Springer; 2005. p. 1–24.
- [2] Pinnavaia T, Beall G. Polymer-clay nanocomposites. Wiley; 2001.
- [3] Hussain F, Hojjati M, Okamoto M, Gorga RE. Review article: polymer-matrix nanocomposites, processing, manufacturing, and application: an overview. *J Compos Mater* 2006;40(17):1511–75.
- [4] Sinha Ray S, Okamoto M. Polymer/layered silicate nanocomposites: a review from preparation to processing. *Prog Polym Sci* 2003;28(11):1539–641.
- [5] Kawasumi M, Hasegawa N, Kato M, Usuki A, Okada A. Preparation and mechanical properties of polypropylene-clay hybrids. *Macromolecules* 1997;30(20):6333–8.
- [6] Akane O, Arimitsu U. Twenty years of polymer-clay nanocomposites. *Macromol Mater Eng* 2006;291(12):1449–76.
- [7] Alexandre M, Dubois P. Polymer-layered silicate nanocomposites: preparation, properties and uses of a new class of materials. *Mater Sci Eng R* 2000;28(1–2):1–63.
- [8] Khatua BB, Lee DJ, Kim HY, Kim JK. Effect of organoclay platelets on morphology of nylon-6 and poly(ethylene-ran-propylene) rubber blends. *Macromolecules* 2004;37(7):2454–9.
- [9] Frounchi M, Dadbin S, Salehpour Z, Noferesti M. Gas barrier properties of PP/EPDM blend nanocomposites. *J Membr Sci* 2006;282(1–2):142–8.
- [10] Gonzalez I, Eguiazabal JI, Nazabal J. New clay-reinforced nanocomposites based on a polycarbonate/polycaprolactone blend. *Polym Eng Sci* 2006;46(7):864–73.
- [11] Wang Y, Zhang Q, Fu Q. Compatibilization of immiscible poly(propylene)/polystyrene blends using clay. *Macromol Rapid Commun* 2003;24(3):231–5.
- [12] Kelarakis A, Giannelis EP, Yoon K. Structure-properties relationships in clay nanocomposites based on PVDF/(ethylene-vinyl acetate) copolymer blends. *Polymer* 2007;48(26):7567–72.
- [13] Hong JS, Kim YK, Ahn KH, Lee SJ. Shear-induced migration of nanoclay during morphology evolution of PBT/PS blend. *J Appl Polym Sci* 2008;108(1):565–75.
- [14] Zhang J, Hereid J, Hagen M, Bakirtzis D, Delichatsios MA, Fina A, et al. Effects of nanoclay and fire retardants on fire retardancy of a polymer blend of EVA and LDPE. *Fire Safety J* 2009;44(4):504–13.
- [15] Fornes TD, Hunter DL, Paul DR. Nylon-6 nanocomposites from alkylammonium-modified clay: the role of alkyl tails on exfoliation. *Macromolecules* 2004;37(5):1793–8.
- [16] Hong JS. The role of organically modified layered silicate in the breakup and coalescence of droplets in PBT/PE blends. *Polymer* 2006;47:3967–75.
- [17] Lee KM, Han CD. Effect of hydrogen bonding on the rheology of polycarbonate/organoclay nanocomposites. *Polymer* 2003;44(16):4573–88.
- [18] Urbanczyk L, Calberg C, Benali S, Bourbigot S, Espuche E, Gouanve F, et al. Poly(ϵ -caprolactone)/clay masterbatches prepared in supercritical CO₂ as efficient clay delamination promoters in poly(styrene-co-acrylonitrile). *J Mater Chem* 2008;18(39):4623–30.
- [19] Urbanczyk L, Calberg C, Stassin F, Alexandre M, Jérôme R, Jérôme C, et al. Synthesis of PCL/clay masterbatches in supercritical carbon dioxide. *Polymer* 2008;49(18):3979–86.
- [20] Stretz HA, Paul DR. Properties and morphology of nanocomposites based on styrenic polymers. Part I: styrene-acrylonitrile copolymers. *Polymer* 2006;47(24):8123–36.
- [21] Vaia RA, Liu W. X-ray powder diffraction of polymer/layered silicate nanocomposites: model and practice. *J Polym Sci, Part B: Polym Phys* 2002;40(15):1590–600.
- [22] Benali S, Peeterbroeck S, Larrieu J, Laffineur F, Pireaux J-J, Alexandre M, et al. Study of interlayer spacing collapse during polymer/clay nanocomposite melt intercalation. *J Nanosci Nanotechnol* 2008;8:1707–13.
- [23] Kim WY, Lee DS. Morphology and mechanical property of the polycarbonate poly(styrene-co-acrylonitrile) blend containing poly(ϵ -caprolactone). *Polym Bull* 1991;26(6):701–7.